ISSN 2616-5767 Vol.5, Issue 5: 1-6, DOI: 10.25236/AJETS.2022.050501

Interpretation properties of geological radar for ionized rare-earth based on model experiment

Xia Wu*

School of Architecture Engineering, Jiangxi College of Applied Technology, Ganzhou, 341000, China
**Corresponding author:2181049849@qq.com*

Abstract: *Ionized rare-earth is a special kind of soil, which contains free ions soluble in water, and its conductivity is affected by both ion concentration and water content. Mastering the waveform properties of geological radar in this kind of soil layer under different water content conditions is helpful to improve the accuracy of post-interpretation. To obtain the interpretation properties, the model experiment was proposed. Firstly, the rectangular model box was prepared by self-made, and filled with on-site soil samples. Then, the water content of the model fill was controlled by manual configuration, and the waveform image was obtained by detecting the model fill with geological radar. Furtherly, The IDSP interpretation program was used to pre-process the waveform image, such as filtering and energy gain. The results show that when the water content is more than 30%, the electromagnetic loss is significant and the reflection intensity is sharply reduced, meanwhile the spectrum energy is concentrated with obvious low frequency, and the main frequency distribution range is 150-400MHz. The results can provide relevant reference for geological radar detection in ionized rare-earth.*

Keywords: *Ionized rare-earth, Geological radar, Model experiment, Water content, Post-interpretation*

1. Introduction

Compared with common soil, ionized rare-earth contains soluble free ions, and the conductivity of soil layer is affected by water content and free ions at the same time, and free water promotes the solubility [1]. Therefore, the relative permittivity of ionized rare-earth is not only affected by water content, but also related to the concentration of free ions. In this case, it is difficult to obtain accurate and reliable relative permittivity and corresponding interpretation properties by using existing calibration techniques.

To solve this problem, some scholars proposed a method to calculate the relative permittivity of ionized rare-earth by establishing a dielectric model of mixed medium based on multifactor coupling analysis, e.g., relying on a road base in Alatan area, Xu [2] carried out the freeze-thaw cycle test of water-salt migration, and established the fitting formula between relative permittivity and multifactor under the condition of positive temperature by regression analysis. To calculate the relative permittivity of gravel sulphate ionized rare-earth under different water content and temperature conditions, Lei et al. [3] established the linear fitting equations between water content, salt content and real and imaginary parts of composite permittivity based on Dobson permittivity correction model, and obtained the empirical formula. Wu et al. [4] introduced saturation into the Stogryn dielectric model and analyzed the dielectric characteristics of soil samples with different water content and salt content based on the control test. After statistical regression analysis and field verification, a modified model that was more suitable for high water content conditions was given. It was found that when the water content, ions content and porosity were known, the accuracy of calculation results could be improved by this modified model. There is no doubt that the calculation models of permittivity of such mixed media can make up for certain deficiency to some extent.

However, in order to ensure the accuracy of the calculation results, it is necessary to accurately calculate the volume ratio of each component, the concentration of free ions, air temperature, and volumetric water content in the practical application of the permittivity calculation model of the above mixed medium. For on-site detection, it is not easy to obtain these parameters, so it is difficult to meet the requirements of rapidity and timeliness in engineering practice.

In this regard, based on an ionized rare-earth natural site in Jiangxi province, China, this paper

ISSN 2616-5767 Vol.5, Issue 5: 1-6, DOI: 10.25236/AJETS.2022.050501

proposes to use indoor model experiment to analyze the waveform properties of geological radar so as to provide reasonable and useful information for post-interpretation.

2. Project Introduction

This site is located in Xiaoping Township, Ganzhou City, about 95 km away from the urban area. It was discovered by local workers when they collected crystal in the early 19th century. The lithology of the strata is mainly limestone, granite and slate, with obvious folds and faults. The two wings of the folds are narrow and the east wing is wider, and the dip angle of the strata is 25 ~ 35 °. In addition, rock mass is exposed on the west side of the site, and there are 8 fault structures in the area, in which, the F1 fault structure has a length of 16 km and an inclination of 65 ~ 75 °, which is a huge compression-torsion fault. The contact between the upper and lower walls forms a breccia belt with a thickness of tens of meters, which directly controls the vertical distribution of No.22 and No.23 ore-bearing skarns.

Since its discovery, the site has been using in-situ leaching technology for rare-earth extraction. Due to the long-term lack of efficient and environmentally-friendly extraction technology and neglect of supervision, the phenomenon of indiscriminate excavation and illegal mining has always existed, resulting in serious rare-earth extraction wastewater pollution in the surrounding mountains, farmland and rivers within tens of kilometers. Figure 1 show the excavation site, which shows that the hill and soil have suffered serious damage.

Figure 1: Excavation site

With the adjustment of rare-earth policy and the increase of industry control, the phenomenon of indiscriminate digging and mining has been effectively curbed. However, the surrounding mountains and farmland have been polluted to varying degrees. Since the spring of 2020, the local environmental protection has been continuously strengthened, and the local government has begun to rectify and repair the pollution. In order to provide reliable reference information for subsequent mountain pollution treatment, the site management office introduced the geological radar in June 2021 to detect the stratum to find out the pollution range.

3. Model Experiment

When determining the size of the model box, it is necessary to take the effective detection depth of the geological radar and the convenience of manufacturing and handling into consideration. The final size is 3.0m × 1.0m × 1.0 m in length × width × height.

Metal materials will interfere with the electromagnetic wave emitted by geological radar antenna and cause false signals in the detection image. Therefore, the material of the model box must be non-metallic products. At last, the high density composite plate was selected, and the waterproof paint was applied to the inside surface of the box to prevent the plate from absorbing the water of the filler. In addition, the plain loess was selected as the parent soil of the filling. Firstly, the soil samples need to be salt-washed and dried to reduce the uncertainty influence of other ions or salts on the experimental results. Then, the water ratio and ions content of the filling were prepared by manual [5]. According to the measured data of water ratio and ions content in the geotechnical center laboratory, the water ratio

ISSN 2616-5767 Vol.5, Issue 5: 1-6, DOI: 10.25236/AJETS.2022.050501

range of the model fill was 30%-45%, and the ions content ratio of 100g dry soil was 0.3%-1.0%. According to the local meteorological and climatic data, the temperature of the model fill was controlled in a positive temperature state by the laboratory temperature controller, ranging from 12-37 ℃. When entering the box, it was divided into 4 layers according to the design compaction degree, and the thickness of each layer was 25 cm.

After filling the model, the geological radar with type of LK200 equipped with 600MHz emitting antenna was used to detect the model box to obtain the waveform images. In addition, in order to facilitate the analysis and statistics, the detection files were also numbered and the corresponding water ratio was recorded each time.

4. Interpretation Properties

After analysis, it found that when the water content is more than 30%, the electromagnetic wave reflection intensity will rapidly weaken or even fail to produce effective reflection, which is manifested in two aspects: First, there will be a large number of fuzzy signals in detected images, which do not have a continuous and stable shape, and the change of in-phase axis is irregular, so it is difficult to implement discrimination and interpretation; Second, the reflection intensity drops sharply, and only a small number of distinguishable reflection signals can be seen in the shallow layer near the soil surface in the line-scan image. With the increase of depth, the reflection signals can't be distinguished, and the waveform amplitude in point-scan image is very small. If the water ratio continues to increase, the whole waveform will become approximately horizontal straight line.

The main frequency of reflected echo has obvious low-frequency characteristics, and its distribution range is 150-400MHz, which is about 1/4-3/4 of the central frequency of the incident electromagnetic wave. At the same time, the amplitude of main frequency curve is small and the spectrum is concentrated, which indicates that the energy attenuation is severe and the high frequency wavelet has been preferentially absorbed.

Figure 2 shows the line-scan detected image when the water content (ω) is 32%. It can be seen that there are relatively stable and continuous reflection signals in the depth range of 0-35cm. Although the in-phase axis is messy, the signals are relatively uniform and uninterrupted, which can be interpreted. When the buried depth exceeds it, the signal becomes extremely fuzzy, and a large number of spots appear, and there is no discernible signal. Moreover, the greater the depth, the more spots are displayed, which makes it difficult to analyze.

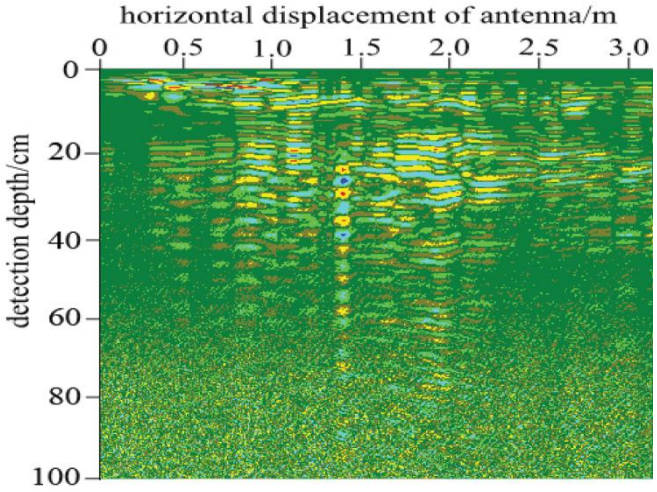

Figure 2: Line-scan image (ω=32%)

Figure 3 shows the line-scan image when ω=45%. It is found that the continuous and stable reflection signal can be seen only within the range of 10cm, and when the depth is exceeded, the signal is interrupted and there are also a lot of spots, which indicates that the attenuation of electromagnetic energy is more serious.

It should be noted that a fuzzy horizontal reflection signal can be seen at the depth of 40cm and continues to 70cm. This reflection signal is not generated by the soil layer but by the metal measuring instrument, which needs to be distinguished. In addition, the measuring instrument is made of metal

ISSN 2616-5767 Vol.5, Issue 5: 1-6, DOI: 10.25236/AJETS.2022.050501

material. If it is in a dry soil layer, it will generate a strong, continuous and stable reflection signal [6, 7], but its reflection signal is still vague in this figure, which indicates that the electromagnetic waves have produced huge energy loss in the environment with high water ratio.

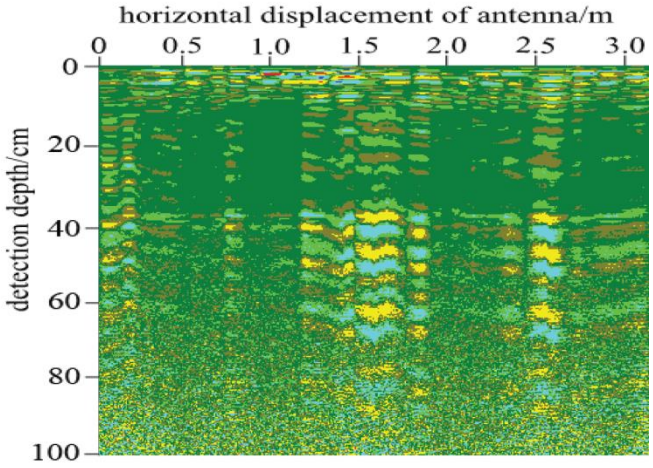

Figure 3: Line-scan image (ω=45%)

Figure 4 shows the point-scan image and echo main frequency curves corresponding to Figure 3. It is easy to find that the waveform amplitude in the point-scan image is small. Except for the obvious amplitude in the range of 0-10cm, the waveform in other depth ranges is approximately a horizontal straight line with slight amplitude, which is consistent with the features shown in Figure 3. As can be seen in Figure 4 (*b*), the main frequency of the echo is low and prominent and the spectrum energy is concentrated.

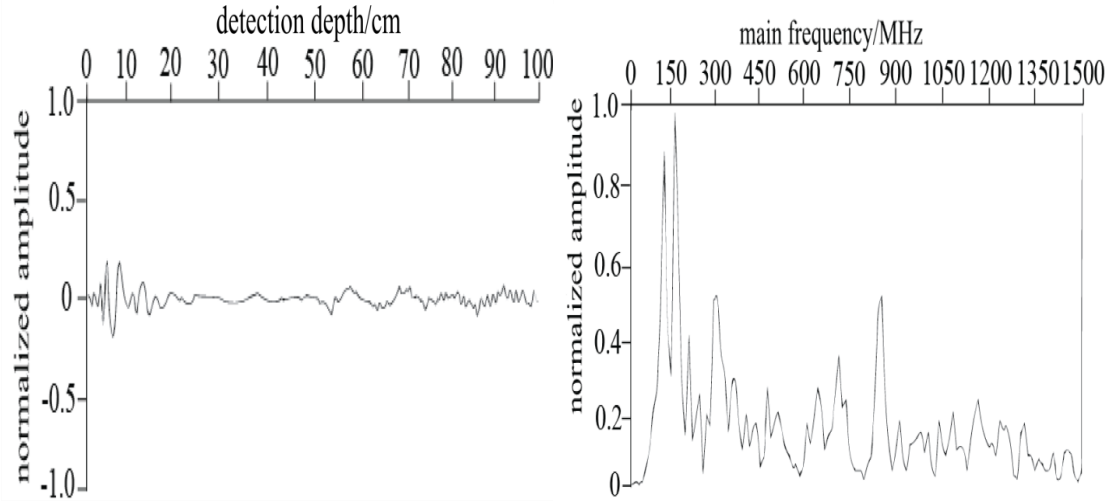

(a) Point-scan image *(b) Echo main frequency curve*

Figure 4: Point-scan image and echo main frequency curve (ω=45%)

5. Discussion

The incident electromagnetic wave emitted by radar antenna is essentially composed of sequence wavelets. The sequence wavelets have the same initial energy and phase velocity of transmission, but the initial frequencies of different wavelets are different. After synthesis, the central frequency of the incident electromagnetic wave can be obtained [8, 9]. When the incident electromagnetic wave propagates in the medium, different wavelets have electromagnetic polarization coupling, and the wavelets with high frequency have the advantage of coupling. The existence of water causes water molecules to wrap the soil particles, thus forming more water films on the surface of the soil particles, which can promote the microscopic movement of the soil particles and the conduction of the electric field [10-13]. Obviously, this accelerates the coupling and transmission efficiency between micro electromagnetic fields, i.e. enhances the degree and efficiency of electromagnetic polarization.

ISSN 2616-5767 Vol.5, Issue 5: 1-6, DOI: 10.25236/AJETS.2022.050501

However, high-frequency wavelets have the coupling advantage, which leads to the high-frequency wavelets being preferentially absorbed in the environment with high water ratio, so that the reflected echo is mainly low-frequency wavelets.

In addition, the content of free ions increases rapidly and the speed of dispersion movement is faster in the environment of high water ratio. Free ions themselves belong to charged particles. Due to the adsorption of water film on the surface of soil particles, a large number of free ions are adsorbed on the surface of soil particles to form charged particle clusters [14, 15]. The electromagnetic field intensity of charged particle clusters is stronger and its influence range is wider. When coupled with wavelet, it will produce great potential difference, weaken wavelet energy and lead to serious energy loss. In this situation, even if the signal receiver can receive the reflected echo, its energy is already very weak, and it can't produce effective interpretation signal, which is characterized by fuzzy spots.

To sum up, under the condition of normal temperature, the high water ratio in the soil layer and the increase of free ion concentration caused by it are the key factors leading to weak reflection and low frequency characteristics. The above research results are basically consistent with theoretical analysis, and should be paid attention to in future research and practical work.

6. Conclusions

(1) When the water content is more than 30%, the reflection intensity decreases sharply and there are a large number of fuzzy speckle signals in line-scan detection images, which is difficult to implement effective interpretation and analysis. The waveform amplitude in point-scan detection images is weak and even presents the characteristics of approximate horizontal straight line. The spectrum energy is concentrated and the low-frequency characteristics are obvious with a distribution range of 150-400MHz.

(2) Special attention should be paid to the water content of the soil layer when geological radar detection is adopted. Under the condition of high water ratio, its applicability is poor, which is probably difficult to provide effective reference information for engineering practice and it needs to be selected carefully.

Acknowledgements

This work was supported in part by the Science and Technology Research Project of the Education Department of Jiangxi Province under Grant GJJ204903.

References

[1] Chu, W. Schroeder, D.M; Siegfried, M.R. Retrieval of Englacial Firn Aquifer Thickness From Ice-Penetrating Radar Sounding in Southeastern Greenland. Geophys Res Lett. 2018, 45, 11770-11778.

[2] Xu, S. Study on the Law of Dielectric Constants and Water and Salt Transport in Unsaturated Soils under Freezing and Thawing. Master Thesis. Northeast Forestry University, Harbin, China, 2018.

[3] Lei, L. Tiyip, T. Ding, J.L. Jiang, H.N. Yao, Y. Sun, Y.M. Xia, J. Kelimu, A. Constant characteristic and model verification of saline soil dielectric in arid area. Trans. Chin Soc Agr Eng. 2013, 29, 125-133.

[4] Wu, Y. R. Wang, W. Z. Zhao, S. J. Liu, S. H. Dielectric Properties of Saline Soils and an Improved Dielectric Model in C-Band. IEEE Trans Geosci Remote. 2015, 53, 440-452.

[5] Zhang, S.S. Wang, Y.W. Yang, X.H. Wang, L. Zhang, W.W. Zhang, X.L. Simplified predication model of salt expansion rate for gravel sulfite saline soil. Chin. J. Highway Transport. 2015, 28, 1-7+14.

[6] Wu, F.S. Hua, X.M. Study of High Precision Forward Recognition of Cavities behind Tunnel Lining based on Ground Pene-trating Radar. Tunn Constr. 2017, 37, 13-19.

[7] Liu, G.S. Yang, H.D. Tang, J.C. Numerical investigation for responses of electrical logging−while−drilling in complex for-mations. J. Cent South Univ (Sci Technol). 2013, 44, 656-661.

[8] Wang, Z.G. Jin, J. Breswter angle and phase loss of electromagnetic waves at interface between dielectric and metamaterial. J. TONGJI Univ. 2015, 43, 938-943.

[9] Zajicova, K. Chuman, T. Application of ground penetrating radar methods in soil studies: A review. Geoderma. 2019, 343, 116-129.

ISSN 2616-5767 Vol.5, Issue 5: 1-6, DOI: 10.25236/AJETS.2022.050501

[10] Zhao, W. Comparison of Application Efficient of Several Common Electromagnetic Wave CT Imaging Methods. Chin. J. Eng Geophys. 2019, 16, 749-754.

[11] Lee, J.S. Yu, J.D. Non-destructive Method for Evaluating Grouted Ratio of Soil Nail Using Electromagnetic Wave. J. Nondestruct Eval. 2019, 38, 1-15.

[12] Zhou, Q. Jiang, Y. Optimized Transmission Model of Electromagnetic Wave in Underground Coal Mine Based on Particle Swarm Optimization. Coal Technol. 2019, 38, 160-162.

[13] Levatti, H.U. Prat, P.C. Ledesma, A. Cuadrado, A. Cordero, J.A. Experimental Analysis of 3D Cracking in Drying Soils Using Ground-Penetrating Radar. Geotech Test J. 2017, 40, 221-243.

[14] Wen, S.R. Wu, X. Dang, J.T. Qiu, Y.J. Ground Penetrating Radar Advanced Detection and Interpretation of saline soil. Central South University Press, Changsha, China, 2021.

[15] You, J. Qi, Y.M. Shao, G.Y. Ma, C. Yang, Y.Q. Pei, Y.F. Hydrochemical Characteristics and Main Ion Sources of Shallow Groundwater in Zihe River Source Region, Shandong, China. J. Guangxi Norm Univ (Nat Sci Ed.). 2020, 38, 132-139.